Journal of Organometallic Chemistry xxx (2013) 1–7

Contents lists available at ScienceDirect

Journal of Organometallic Chemistry

journal homepage: www.elsevier.com/locate/jorganchem

Catalytic olefin epoxidation with a carboxylic acid-functionalized cyclopentadienyl molybdenum tricarbonyl complex

Ana C. Gomes [a], Sofia M. Bruno [a], Marta Abrantes [b], Clara I.R. Magalhães [a], Isabel S. Gonçalves [a], Anabela A. Valente [a], Martyn Pillinger [a,*]

[a] Department of Chemistry, CICECO, University of Aveiro, Campus Universitário de Santiago, 3810-193 Aveiro, Portugal
[b] Centro de Química Estrutural, Complexo Interdisciplinar, Instituto Superior Técnico, Universidade de Lisboa, Av. Rovisco Pais, 1, 1049-001 Lisboa, Portugal

ARTICLE INFO

Article history:
Received 30 September 2013
Received in revised form
18 October 2013
Accepted 21 October 2013

Dedicated to Prof. Maria José Calhorda on the occasion of her 65th birthday and in recognition of her outstanding contributions to the field of computational organometallic chemistry.

Keywords:
Molybdenum
Cyclopentadienyl ligands
Carbonyl ligands
Layered double hydroxides
Epoxidation
Ionic liquids

ABSTRACT

The complex $CpMo(CO)_3CH_2COOH$ (**1**) (Cp = η^5-C_5H_5) has been examined as a precatalyst for the epoxidation of *cis*-cyclooctene and α-pinene using *tert*-butylhydroperoxide (TBHP) as oxidant. A high turnover frequency of ca. 600 mol mol_{Mo}^{-1} h^{-1} was achieved in the epoxidation of cyclooctene, giving the epoxide as the only reaction product. With α-pinene as substrate, the added-value products α-pinene oxide and campholenic aldehyde were obtained. Two different approaches to facilitate catalyst recovery and reuse were explored: (1) use of an ionic liquid (IL) as solvent, and (2) intercalation of **1** in a Zn,Al layered double hydroxide (LDH) by a direct synthesis (coprecipitation) route. Characterization of the LDH by powder X-ray diffraction, thermogravimetric analysis, FT-IR and ^{13}C CP MAS NMR spectroscopies showed that the $CpMo(CO)_3CH_2COO^-$ anions intercalate in a bilayer arrangement, resulting in an interlayer spacing of 20.7 Å. In the epoxidation of cyclooctene, catalytic activity in the first batch run was very high for the catalyst/IL mixture and moderate for the LDH. Characterization of the LDH after catalysis indicated that nearly complete oxidative decarbonylation of supported complexes had occurred (by reaction with TBHP), resulting in the presence of immobilized oxomolybdenum species. However, catalytic activities for both the recovered LDH and catalyst/IL decreased in consecutive runs, due in part to progressive removal of active species during either the catalytic reaction (for the LDH) or the solvent extraction/work-up (for the catalyst/IL mixture).

1. Introduction

The epoxidation of olefins catalyzed by molecular transition metal compounds continues to be a topic of considerable academic and industrial interest [1–3]. Molybdenum-based catalysts have been widely used in this reaction. The well known industrial example is the Arco-Lyondell process for the epoxidation of propene using $Mo(CO)_6$ as a precursor, which is oxidized *in situ* by the oxidant *tert*-butylhydroperoxide (TBHP) to give the active molybdenum(VI) catalyst [4–6]. During the last decade there has been increasing interest in the use of cyclopentadienyl molybdenum carbonyls of the type $Cp'Mo(CO)_3X$ (Cp′ = η^5-C_5R_5 (R = H, alkyl, *ansa*-bridge); X = halide, alkyl, *ansa*-bridge) as precatalysts for olefin epoxidation [7,8]. Great variability by ligand modification (both on the Cp-ring and directly at the metal center) is possible, opening the way to immobilization [9,10] and chirality introduction [11,12]. Based on catalytic activities obtained for the epoxidation of *cis*-cyclooctene (used as a benchmark substrate), standout precatalysts include (η^5-C_5Bz_5)$Mo(CO)_3Cl$ (Bz = benzyl) [13], the *ansa*-complex [Mo(η^5-$C_5H_4(CH(CH_2)_3)$-η^1-CH)$(CO)_3$] (with a room temperature ionic liquid (RTIL) as a solvent) [14], and the fluorinated complex $CpMo(CO)_3CF_3$ (with hexafluoroisopropanol as a solvent; Cp = η^5-C_5H_5) [15]. These tricarbonyl complexes undergo oxidative decarbonylation *in situ* by reaction with TBHP, forming catalytically active Mo-oxo, $Cp'MoO_2X$, and Mo-oxo-peroxo, $Cp'MoO(\eta^2$-$O_2)X$, species. More complex species may also be formed as in the analogous oxidation of $(CpBz)Mo(CO)_3Me$ that gives $[(CpBz)MoO_2]_2(\mu$-O) [16]. Computational studies support a mechanism in which active intermediates of the type $Cp'MoO(OH)(OO^tBu)X$ and $Cp'Mo(\eta^2$-$O_2)(OH)(OO^tBu)X$ are formed by reaction of the respective Mo-oxo and Mo-oxo-peroxo complexes with excess TBHP [17,18].

In the present study the complex $CpMo(CO)_3CH_2COOH$ (**1**) has been prepared, characterized, and examined as a precatalyst for the epoxidation of *cis*-cyclooctene and α-pinene. The recovery and reuse of the homogeneous catalyst was explored using an ionic

* Corresponding author. Fax: +351 234 401470.
E-mail address: mpillinger@ua.pt (M. Pillinger).

0022-328X/$ – see front matter © 2013 Elsevier B.V. All rights reserved.
http://dx.doi.org/10.1016/j.jorganchem.2013.10.037

liquid as a solvent. Additionally, a new approach for the immobilization of cyclopentadienyl molybdenum tricarbonyl complexes is reported, based on the intercalation of **1** in a layered double hydroxide.

2. Experimental

2.1. Materials and methods

Microanalyses for CHN and ICP-OES analysis for Mo were determined by C.A.C.T.I., University of Vigo. Powder X-Ray diffraction (XRD) data were collected at room temperature on an X'pert MPD Philips diffractometer with a curved graphite monochromator (Cu-K_α radiation, $\lambda = 1.54060$ Å) and a flat-plate sample holder, in a Bragg–Brentano para-focusing optics configuration (45 kV, 50 mA). Samples were step-scanned in 0.02° 2θ steps with a counting time of 50 s per step. SEM with coupled EDS was carried out on a Hitachi SU-70 (S-4100) instrument using a 15 kV accelerating voltage. Thermogravimetric analysis (TGA) was performed using a Shimadzu TGA-50 system at a heating rate of 5 °C min^{-1} under air. FT-IR spectra were obtained as KBr pellets using an FTIR Mattson-7000 spectrophotometer and recorded from 4000 to 350 cm^{-1}. Raman spectra were recorded on a Bruker RFS100/S FT instrument (Nd:YAG laser, 1064 nm excitation, InGaAs detector). Liquid-state ^1H and ^{13}C NMR spectra were measured with a Bruker Avance 300 instrument. Solid-state NMR spectra were recorded on a Bruker Avance 400 spectrometer. ^{13}C cross polarization (CP) magic-angle spinning (MAS) NMR spectra were recorded at 100.62 MHz with 3.3 μs ^1H 90° pulses, a 2 ms contact time, a spinning rate of 12 kHz and 4 s recycle delays. Chemicals shifts are quoted in ppm relative to TMS. ^{27}Al MAS NMR spectra were recorded at 104.26 MHz using a π/12 pulse of 0.78 μs, a spinning rate of 14 kHz and 1 s recycle delays. Chemicals shifts are quoted in ppm relative to $[Al(H_2O)_6]^{3+}$.

Where appropriate, preparations and manipulations were carried out using standard Schlenk techniques under nitrogen. The chemicals sodium (Riedel-de-Haën), dicyclopentadiene (BDH), $Mo(CO)_6$ (Fluka), 2-chloroacetamide ($ClCH_2CONH_2$, 98%, Sigma–Aldrich), anhydrous *n*-pentane (95%, Sigma–Aldrich), anhydrous tetrahydrofuran (THF, 99.9%, Sigma–Aldrich), anhydrous chloroform (99%, Sigma–Aldrich), acetone (99%, Sigma–Aldrich), hydrochloric acid (HCl, 37%, Fluka), zinc nitrate hexahydrate (99%, Fluka), aluminum nitrate nonahydrate (98.5%, Riedel-de-Haën), 50% aqueous sodium hydroxide (Fluka), Na_2CO_3 (J.M. Vaz Pereira), and 1-butyl-3-methylimidazolium bis(trifluoromethylsulfonyl)imide ([bmim]NTf_2, 99%, io-lo-tec) were obtained from commercial sources and used as received. The solution of *tert*-butylhydroperoxide (TBHP) in decane (5–6 M, Sigma–Aldrich, <4% water) was dried over activated 4 Å molecular sieves prior to use. The Zn,Al-NO_3 LDH precursor was prepared by the standard method of coprecipitation of the Zn^{2+} and Al^{3+} hydroxides (initial Zn^{2+}/Al^{3+} molar ratio in solution = 2) in the presence of nitrate ions at constant pH (7.5–8) under nitrogen, followed by aging at 80 °C for 20 h [19]. After washing, the material was stored as an aqueous suspension in a closed container.

2.2. Synthesis

2.2.1. $CpMo(CO)_3CH_2COOH$ (**1**)

$CpMo(CO)_3CH_2COOH$ (**1**) was synthesized according to the general procedure described by Ariyaratne et al. [20]. A detailed description of the preparation is given here. Freshly cut sodium (0.78 g, 34.0 mmol) was added to 40 mL of dicyclopentadiene under inert atmosphere. The mixture was refluxed overnight at 160 °C. The resultant suspension was filtered and the remaining pink solid residue (NaCp) washed with anhydrous *n*-pentane (2 × 15 mL) and vacuum-dried. NaCp was treated overnight with $Mo(CO)_6$ (5.40 g, 20.4 mmol) in refluxing THF (60 mL). The resultant reaction mixture was cooled to room temperature and $ClCH_2CONH_2$ (1.91 g, 20.4 mmol) in THF (60 mL) added. After stirring at room temperature for 2 h, the brown suspension was vacuum-dried and the resultant residue extracted with chloroform. The chloroform fractions were combined and evaporated to dryness, giving $CpMo(CO)_3CH_2COONH_2$, which was subsequently treated with water (34 mL) and HCl (37%, 12 mL, ca. 140 mmol) at 80 °C for 1 h. $CpMo(CO)_3CH_2COOH$ (**1**) precipitated as a yellow powder, which was filtered, washed with water, vacuum-dried, and recrystallized from chloroform (1.30 g, 21%, relative to $Mo(CO)_6$). Anal. Calcd for $C_{10}H_8MoO_5$ (304.11): C, 39.50; H, 2.65. Found: C, 39.2; H, 2.65. FT-IR (KBr, cm^{-1}): ν = 3438 (br), 3120 (w), 2935 (w), 2784 (w), 2624 (w), 2524 (w), 2025 (vs, ν(CO)), 1949 (vs, ν(CO)), 1931 (vs, ν(CO)), 1908 (vs, ν(CO)), 1647 (vs, ν(C=O)), 1427 (m), 1416 (m), 1283 (vs, ν(C–O)), 1104 (m), 1043 (m), 1002 (w), 923 (w), 844 (m), 825 (m), 742 (w), 655 (m), 580 (m), 552 (s), 482 (s), 435 (m), 360 (w). FT-Raman (cm^{-1}) ν = 3129 (m), 3109 (w), 3020 (w), 2959 (w), 2013 (s), 1957 (vs), 1935 (w), 1903 (s), 1110 (s), 1058 (w), 1043 (s), 465 (w), 440 (m), 417 (m), 394 (m), 362 (s), 341 (s), 156 (w), 140 (s), 124 (vs), 112 (vs). ^1H NMR (300 MHz, $CDCl_3$, 298 K): δ = 5.43 (s, 5H, Cp), 1.80 (s, 2H, CH_2COOH). ^{13}C NMR (126 MHz, $CDCl_3$, 298 K): δ = 239.3 (CO), 226.3 (CO), 188.0 (CH_2COOH), 93.8 (Cp), −4.5 (CH_2COOH).

2.2.2. Zn,Al-CpMo

A yellow solution of the sodium salt $[CpMo(CO)_3CH_2COO]Na$ was prepared by addition of 1 equivalent of NaOH to an aqueous suspension (30 mL) of complex **1** (0.46 g, 1.50 mmol). A solution of $Zn(NO_3)_2{\cdot}6H_2O$ (0.59 g, 2.00 mmol) and $Al(NO_3)_3{\cdot}9H_2O$ (0.37 g, 1.00 mmol) in decarbonated deionized (DD) water (30 mL) was then added dropwise, and the pH of the mixture was continuously maintained between 7.5 and 8 using 0.2 M NaOH. After the addition was completed the reaction mixture was aged at 65 °C for 19 h. The resultant yellow solid was filtered, washed extensively with DD water and acetone, and finally vacuum-dried. Anal. found: Mo, 12.7%. FT-IR (KBr, cm^{-1}): ν = 3448 (br), 2017 (vs, ν(CO)), 1950 (vs, ν(CO)), 1909 (vs, ν(CO)), 1633 (m), 1579 (m), 1491 (m), 1429 (m), 1360 (s), 1350 (s), 1261 (vw), 1113 (w), 1060 (w), 1014 (w), 825 (m), 790 (w), 748 (w), 625 (bd), 580 (w), 553 (w), 484 (m), 428 (m). FT-Raman (cm^{-1}): ν = 3119 (m), 2945 (w), 2022 (m), 1944 (m), 1110 (s), 1061 (w), 918 (w), 448 (w), 415 (w), 339 (s), 115 (s). ^{13}C CP MAS NMR: δ = 242.8 (CO), 232.0 (CO), 227.0 (CO), 191.5 ($CH_2CO_2^-$), 177.0 (CO_3^{2-}), 94.0 (Cp), 1.3 ($CH_2CO_2^-$). ^{27}Al MAS NMR: δ = 13.5.

2.3. Catalytic tests

The catalytic reactions were carried out under air (autogenous pressure) and stirred magnetically (1000 rpm) in a closed borosilicate reactor (10 mL capacity) equipped with a valve for sampling, and immersed in an oil bath thermostated at 55 °C. Typically, the reactor was loaded with catalyst (18 μmol of molybdenum), olefin (1.8 mmol, *cis*-cyclooctene (Cy) or α-pinene (Pin)) and 5–6 M TBHP in decane (ca. 2.75 mmol). When stated, 150 μL of [bmim]NTf_2 was used as a cosolvent. The olefin, oxidant and (when used) IL were heated in separate vessels (10 min at the reaction temperature) prior to addition to the reactor (with preheated walls) containing the catalyst. Time zero (i.e., the initial instant of the reaction) was taken as the moment the oxidant was added to the reactor. The leaching tests were performed by separating the solid (at 55 °C) from the reaction mixture after 2 h, using a 0.2 μm PTFE GVS membrane; the filtrate was stirred for a further 22 h at 55 °C. The course of the reactions was monitored using a Varian 3800 GC

Please cite this article in press as: A.C. Gomes, et al., Journal of Organometallic Chemistry (2013), http://dx.doi.org/10.1016/j.jorganchem.2013.10.037

equipped with a BR-5 (Bruker) capillary column (30 m × 0.25 mm; 0.25 μm) and a flame ionization detector, using H_2 as the carrier gas.

3. Results and discussion

3.1. Synthesis and characterization

The reaction of NaCp with $Mo(CO)_6$, followed by addition of 2-chloroacetamide, gave the tricarbonyl complex $CpMo(CO)_3CH_2COONH_2$, which was subsequently hydrolyzed to give yellow $CpMo(CO)_3CH_2COOH$ (**1**), as illustrated in Scheme 1. FT-IR and ^1H NMR data for **1** were in agreement with literature results [20].

In recent work we successfully heterogenized the complexes $[Mo(\eta^3\text{-}C_3H_5)Cl(CO)_2(bpdc)]^{2-}$ and *cis*-$[Mo(CO)_4(bpdc)]^{2-}$ (bpdc = 2,2′-bipyridine-5,5′-dicarboxylate) by using layered double hydroxides (LDH) as supports [19,21]. The former complex was intercalated in a one-pot direct synthesis approach [19], while the latter complex was intercalated by ion exchange of a Zn,Al-NO_3 LDH precursor [21]. Initial attempts to intercalate complex **1** by ion exchange of a Zn,Al-NO_3 LDH with a Zn/Al molar ratio of 2 were unsuccessful (reaction conditions: water as solvent, 50 °C, 6 h): while the IR spectra of the resultant material indicated the presence of complex **1**, the powder XRD pattern was unchanged from that for the starting material, suggesting that the tricarbonyl complex was mainly adsorbed on the external surface of the LDH particles. These materials were not further characterized. Instead, a one-pot coprecipitation method at constant pH was found to give an intercalated LDH (abbreviated as Zn,Al-CpMo) as evidenced by powder XRD, elemental analysis, thermogravimetric analysis, vibrational spectroscopy, and ^{13}C and ^{27}Al MAS NMR. Zn^{2+} and Al^{3+} were chosen as the M^{2+}/M^{3+} combination since Zn,Al-LDHs are prepared (and are stable) at near-neutral pH, thereby providing the best compatibility with the anionic complex $CpMo(CO)_3CH_2COO^-$.

A comparison of the FT-IR spectra for Zn,Al-CpMo and complex **1** confirms the presence of intact $CpMo(CO)_3CH_2COO^-$ anions (Fig. 1). Zn,Al-CpMo displays three very strong ν(CO) bands at 1909, 1950 and 2017 cm^{-1}, similar to those displayed by **1** (1908, 1949 and 2025 cm^{-1}) and in agreement with that reported for other complexes of the type $Cp'Mo(CO)_3X$ [13,20,22,23]. Complex **1** exhibits two very strong bands at 1283 and 1647 cm^{-1}, which are attributed to the C–O and C=O stretching vibrations of the carboxylic acid group. These bands are absent in the spectrum of Zn,Al-CpMo. Instead, bands at 1350 and 1579 cm^{-1} (both absent in the spectrum of **1**) appear and are assigned to ν_s(OCO) and ν_{as}(OCO), respectively, of the deprotonated carboxylate group. Whereas the material Zn,Al-NO_3 contains a very strong band at 1383 cm^{-1} due to the antisymmetric stretching mode ν_3 of nitrate ions, this band is not evident in the spectrum of Zn,Al-CpMo, indicating that the material is essentially free of interference from this anion (which is present in the synthesis mixture due to the use of $Zn(NO_3)_2$ and $Al(NO_3)_3$). Below 750 cm^{-1}, the IR spectrum of Zn,Al-CpMo contains several bands due to the guest species (484, 553 and 580 cm^{-1}) in addition to Zn/Al-OH lattice translation modes that are characteristic of Zn,Al-LDHs (428, 553 and 625 cm^{-1}) [24].

To assess the stability of Zn,Al-CpMo, the sample was deliberately exposed to air for one month. The FT-IR spectrum of the resultant solid was unchanged from that for the freshly prepared sample, indicating that the material is neither oxygen- nor moisture-sensitive.

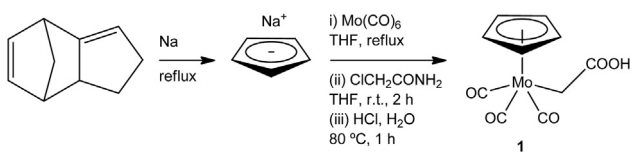

Scheme 1. Synthesis of complex **1**.

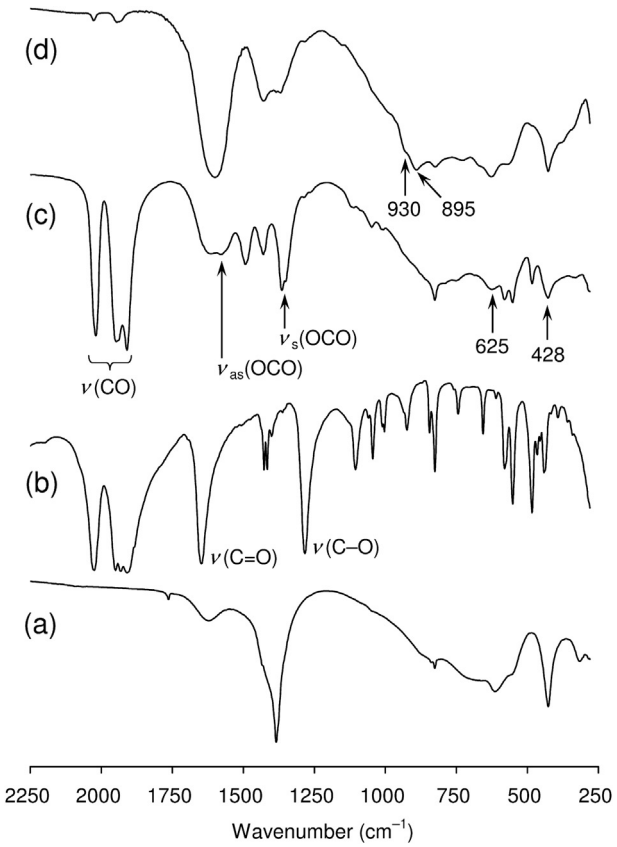

Fig. 1. FT-IR spectra (KBr) of (a) Zn,Al-NO_3, (b) complex **1**, (c) the material Zn,Al-CpMo, and (d) the solid recovered after one batch run of Cy epoxidation using Zn,Al-CpMo as the precatalyst. Selected bands are highlighted.

Fig. 2 compares the ^{13}C CP MAS NMR spectrum of Zn,Al-CpMo with the solution ($CDCl_3$) NMR spectrum of complex **1**. The intercalated LDH shows signals at 1.3 ($CH_2CO_2^-$), 94.0 (Cp), 191.5 ($CH_2CO_2^-$) and 227–243 ppm (CO) for the organometallic guest, and a weak signal at 177.0 ppm that is probably due to carbonate anions. The Cp resonance for Zn,Al-CpMo is unshifted when compared with that for **1** in $CDCl_3$, while the signals for the CH_2 and carboxylate groups are shifted slightly downfield. The ^{27}Al MAS NMR spectrum of Zn,Al-CpMo presents a broad, somewhat asymmetric signal centered at 13.5 ppm that indicates the presence of octahedral aluminum only (Fig. 2).

The thermal decomposition behavior of Zn,Al-CpMo was studied by thermogravimetric analysis under air (Fig. 3). Three weight loss processes can be distinguished up to 325 °C: loss of cointercalated water (20–105 °C, DTG_{max} = 85 °C, 6.6%), loss of CO molecules from the intercalated tricarbonyl complex (105–200 °C, DTG_{max} = 150 °C, 11.7%) and partial dehydroxylation (loss of water) of the hydroxide layers (200–325 °C, DTG_{max} = 265 °C, 9.7%). A further mass loss of 7.3% takes place up to 500 °C, which is attributed to a combination of the further dehydroxylation of the hydroxide layers and the decomposition of the remaining organic moieties. TGA curves were also measured for Zn,Al-NO_3 and complex **1**. Loss of cointercalated water from Zn,Al-NO_3 takes place at a slightly higher temperature (DTG_{max} = 125 °C) than that for Zn,Al-CpMo, while the initial dehydroxylation takes place at the same temperature (DTG_{max} = 265 °C). Complex **1** loses CO molecules abruptly in the temperature range 150–190 °C (DTG_{max} = 170 °C).

Please cite this article in press as: A.C. Gomes, et al., Journal of Organometallic Chemistry (2013), http://dx.doi.org/10.1016/j.jorganchem.2013.10.037

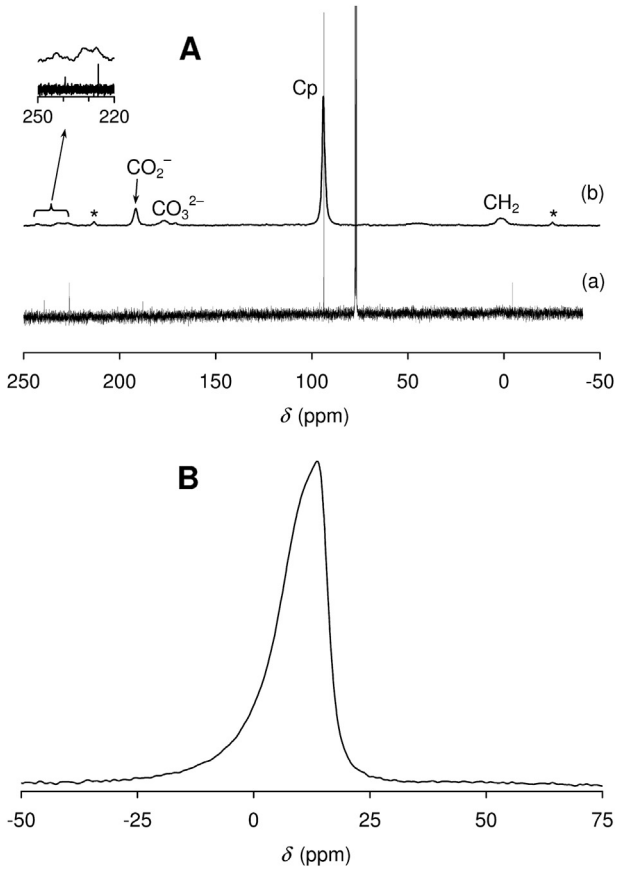

Fig. 2. A. (a) ^{13}C NMR spectrum of **1** in $CDCl_3$. (b) ^{13}C CP MAS NMR spectrum of Zn,Al-CpMo. Spinning sidebands are indicated by asterisks. B. ^{27}Al MAS NMR spectrum of Zn,Al-CpMo.

The second decomposition step occurs between 350 and 500 °C (DTG_{max} = 470 °C), leaving a residual mass of 52.3%. After that, a third mass loss takes place above 650 °C, which could correspond to sublimation of a Mo_xO_y phase. Overall, the TGA results indicate that the thermal behavior of the intercalated complex parallels that of the pure complex **1**. Taking into account the mass losses noted above for Zn,Al-CpMo up to 200 °C, together with the Mo content of 12.7% determined by ICP-OES and the solid state NMR evidence for some carbonate interference, the following formula may be proposed for Zn,Al-CpMo: $Zn_4Al_2(OH)_{12}(CpMo(CO)_3CH_2COO)_{1.5}(CO_3)_{0.25}\cdot 4H_2O$ (calcd: Mo, 13.5%; CO, 11.9%; H_2O, 6.8%).

The powder XRD pattern of Zn,Al-CpMo, recorded at ambient temperature in the range of 3–70° 2θ, presents several reflections that are characteristic of hydrotalcite-like materials (Fig. 4). In particular, the six symmetric, equally spaced peaks found between 3 and 30 °2θ can be assigned as the 00l basal reflections for an expanded phase with an interlayer spacing (d_{003}) of 20.7 Å. Subtraction of 4.8 Å for the thickness of the brucite-like layer gives an interlayer distance (gallery height) of 15.9 Å. This distance is compatible with a bilayer-like arrangement of $CpMo(CO)_3CH_2COO^-$ anions within the interlayer region. Indeed, a similar gallery height of 15.2 Å was previously found for a Zn,Al-LDH intercalated by ferrocenecarboxylate anions (also prepared by coprecipitation from aqueous solution) [25], which were proposed to adopt a bilayer-like arrangement. A bilayer-like arrangement is necessary since these organometallic anions are spatially incapable of balancing the host layer charge of a Zn_2Al-LDH, if arranged in a monolayer. Fig. 5 shows a possible arrangement of $CpMo(CO)_3CH_2COO^-$ anions for which the calculated basal spacing exactly matches the observed value. It is likely that the guest species will be oriented in such a way as to maximize hydrogen-bonding interactions between the carboxylate groups and the layer hydroxyl groups, and position the hydrophobic aromatic groups towards the center of the galleries, as far apart as possible from the hydrophilic layer hydroxyls. In addition to the basal reflections, the powder XRD pattern of Zn,Al-CpMo contains very broad, asymmetric (*hkl*) reflections above ca. 2θ = 30°, characteristic of turbostratic layered structures and/or an intergrowth of the rhombohedral and hexagonal polytypes [26]. The turbostratic effect is caused by a decrease in the ordering along the stacking axis

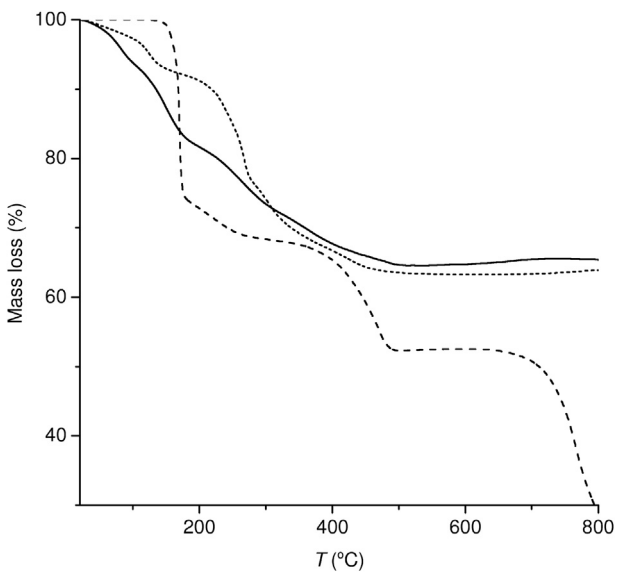

Fig. 3. TGA curves of Zn,Al-CpMo (——), Zn,Al-NO_3 (· · · · ·) and complex **1** (– – –).

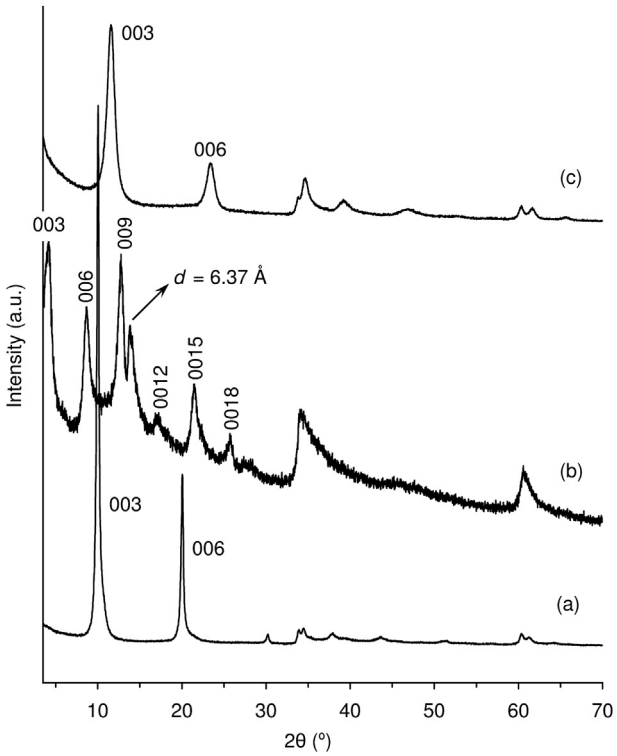

Fig. 4. Powder XRD patterns of (a) Zn,Al-NO_3, (b) Zn,Al-CpMo, and (c) Zn,Al-$ExCO_3$. Selected reflections are assigned.

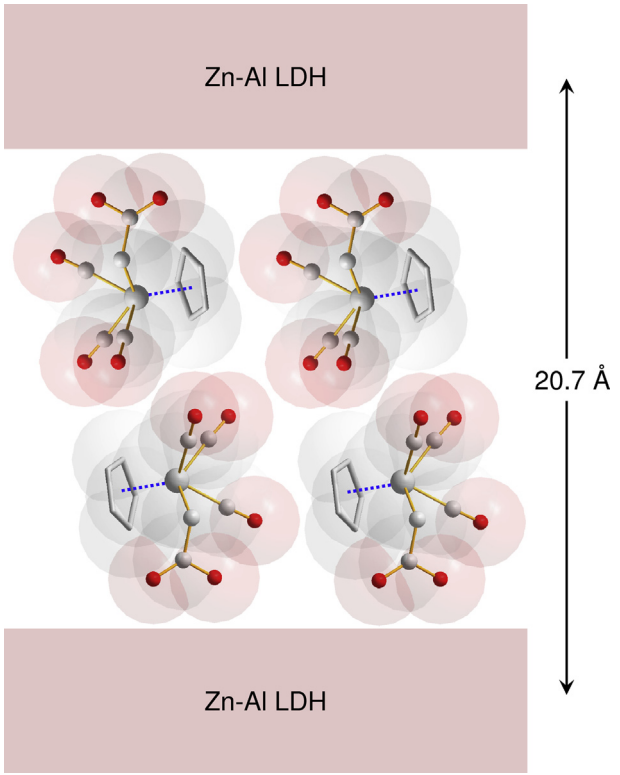

Fig. 5. Model for the interlayer arrangement of $CpMo(CO)_3CH_2COO^-$ anions in the material Zn,Al-CpMo. Van der Waals spheres are drawn for the guest molecules. For simplicity interlayer water molecules have been omitted.

due to the loss of van der Waals interactions between adjacent layers and the absence of a densely packed interlayer space formed by high charge density anions such as carbonate.

The powder XRD pattern of Zn,Al-CpMo contains one additional reflection at $d = 6.37$ Å which is unexpected for an LDH with $d_{003} = 20.7$ Å. We initially assumed that this reflection could be due to an impurity that was not removed during the washing step. To further investigate, a separate experiment was performed in which the material Zn,Al-CpMo (100 mg) was treated with a large excess (ca. 35×) of Na_2CO_3 in water, with the intention of fully exchanging intercalated $CpMo(CO)_3CH_2COO^-$ anions for carbonate anions. After stirring overnight at room temperature, the resultant white solid (referred to as Zn,Al-ExCO_3) was separated from the yellow solution by filtration, washed with water and acetone, and vacuum-dried. The powder XRD pattern of Zn,Al-ExCO_3 is in agreement with patterns reported for Zn,Al-CO_3 LDHs ($d_{003} = 7.64$ Å) [24,27], and neither contains the 00*l* basal reflections for the 20.7 Å phase nor the additional reflection at $d = 6.37$ Å (Fig. 4). Hence we tentatively conclude that the latter reflection may arise due to the periodic distribution of $CpMo(CO)_3CH_2COO^-$ anions within the gallery region.

Fig. 6 shows representative SEM images of Zn,Al-CpMo at different magnifications. The powder comprises irregularly shaped particles which, under higher magnification, revealed an ill-defined morphology that in some regions approximated the classic "sand rose" microstructure. Spatial elemental profiles for Zn, Al and Mo (generated by employing an elemental mapping technique) showed a homogeneous distribution of the elements across the particles.

3.2. Catalytic olefin epoxidation

The epoxidation of *cis*-cyclooctene (Cy) with TBHP in the presence of **1** was very fast and selective, giving 100% cyclooctene oxide (CyO) yield within 30 min, at 55 °C (Fig. 7, Table 1). Under the conditions used the reaction mixture was always homogeneous. In the absence of the molybdenum complex or without TBHP, Cy epoxidation did not take place to a measurable extent throughout 24 h (less than 5% CyO yield), indicating that the simultaneous presence of the molybdenum complex and TBHP is required for catalytic epoxidation. The catalytic activity remained high at nearly ambient temperature, giving 100% conversion within 90 min at 35 °C. The catalytic results for **1** are superior to those reported for other molybdenum tricarbonyl complexes bearing a cyclopentadienyl (Cp) ligand, used as precatalysts in the same reaction under similar conditions. Some reported conversions at 1 h are: 91% for $CpMo(CO)_3(CH_2{-}pC_6H_4{-}CO_2CH_3)$ [28]; ca. 85% for $CpMo(CO)_3Me$ [29]; ca. 95% for $CpMo(CO)_3Cl$ [30]; ca. 65% for $CpMo(CO)_3Et$ [31]. *Ansa*-bridged η^5-cyclopentadienyl molybdenum tricarbonyl complexes led to conversions in the range of 80–100% at 4 h reaction of Cy [31–35].

Complex **1** was further investigated as a precatalyst in the oxidation of α-pinene (Pin) with TBHP, at 55 °C. To the best of our knowledge, there is only one report in the literature on the epoxidation of Pin in the presence of complexes of the type $CpMo(CO)_3X$ (X = Cl [30]). For **1**, the main reaction products were α-pinene oxide (PinOx) and campholenic aldehyde (CPA), and their selectivities depended on the conversion. These two products are used as intermediates or final products in the fragrance [36,37], aroma and pharmaceutical industries [38]. PinOx and CPA were formed in 43%/2% and 5%/35% selectivity, respectively, at 62%/64% conversion, reached at 4 h/24 h reaction. Other reaction products included *trans*-carveol, *iso*-pinocamphone and *trans*-pinocarveol, formed in less than 10% total yield. These products, as well as CPA, may be formed via the isomerization of PinOx [37–39]. The previously studied complex $CpMo(CO)_3Cl$ led to poorer catalytic results: PinOx and CPA selectivities were ca. 20% at 40% conversion, reached at 6 h reaction [30].

Preliminary catalyst stability tests carried out for **1** were very promising. The catalytic activity remained very high when the reagents Cy and TBHP were recharged (in the same amounts as those added initially) to the reactor after the first 24 h run, at 55 °C, leading to 98% CyO yield at 30 min reaction. Hence, the recovery and reuse of the homogeneous catalyst was explored using an ionic liquid (IL) as solvent, namely 1-butyl-3-methylimidazolium bis(trifluoromethylsulfonyl)imide ([bmim]NTf_2). The catalyst/IL mixture was recovered and reused after separating Cy and CyO by solvent extraction, and subsequently adding the reagents Cy and TBHP in amounts equal to those used in the first batch. The catalytic activity was very high, leading to 99% conversion at 10 min reaction, similar to that observed without a cosolvent (Fig. 7, Table 1). These results are superior to those reported for other $CpMo(CO)_3X$/IL systems, tested in the same reaction under similar reaction conditions: $CpMo(CO)_3CF_3$/[bmim]NTf_2 led to 93% conversion at 24 h [15]; $CpMo(CO)_3Me$/[bmim]BF_4 led to ca. 55% conversion at 1 h [29]; $CpMo(CO)_3Me$/[bmim]NTf_2 led to ca. 13% conversion at 1 h, and $CpMo(CO)_3Cl$/[bmim]NTf_2 led to 58% conversion at 4 h [40]. For the **1**/[bmim]NTf_2 system, the reaction rate decreased in consecutive batch runs (Table 1). These results may be partly due to the gradual removal of active species during the solvent extraction process. Similar effects have been reported for the catalytic system $CpMo(CO)_3Me$/[bmim]BF_4 (removal of active species during solvent extraction of the reaction products, accounting for a drop in reaction rate in consecutive batch runs) [29]. The system $CpMo(CO)_3CF_3$/[bmim]NTf_2 led to similar CyO yield for 8 consecutive runs; no description of the recycling procedure was given, making it difficult to carry out comparative studies [15].

In a different approach to improve the catalyst recovery and reuse, complex **1** was immobilized in a Zn,Al layered double

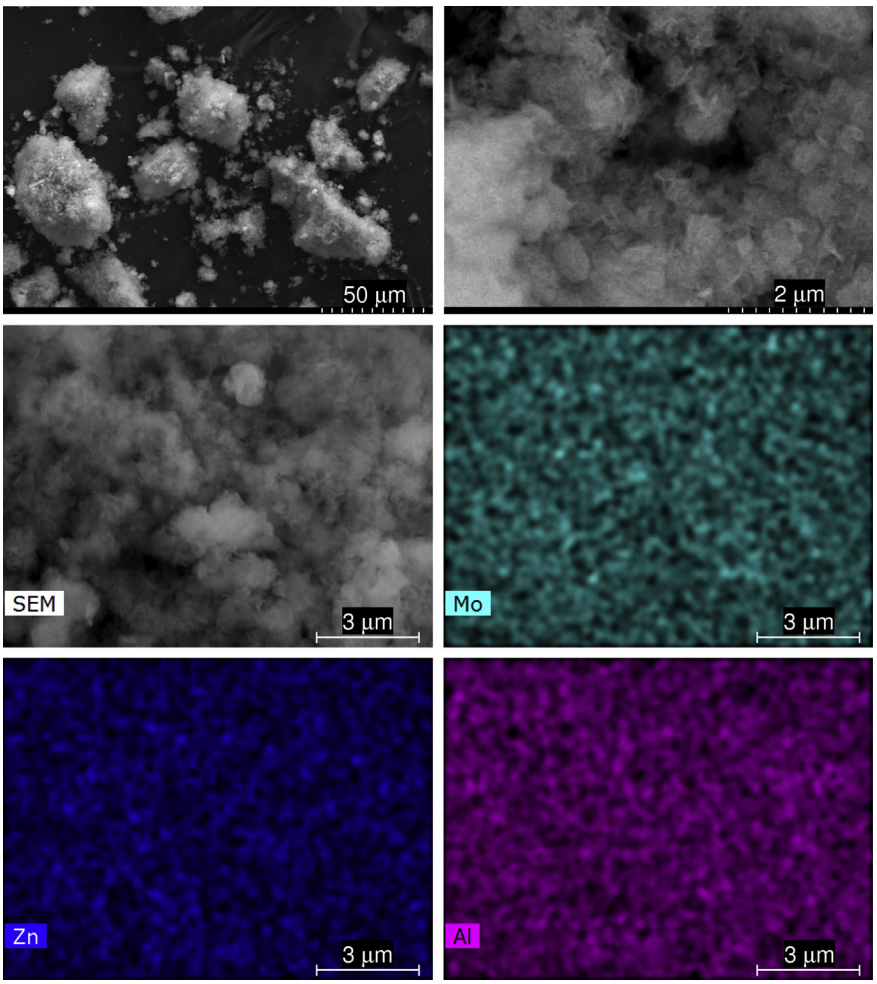

Fig. 6. SEM images of Zn,Al-CpMo. The EDS mapping microimages for the elements Zn, Al and Mo correspond to the SEM image labeled "SEM".

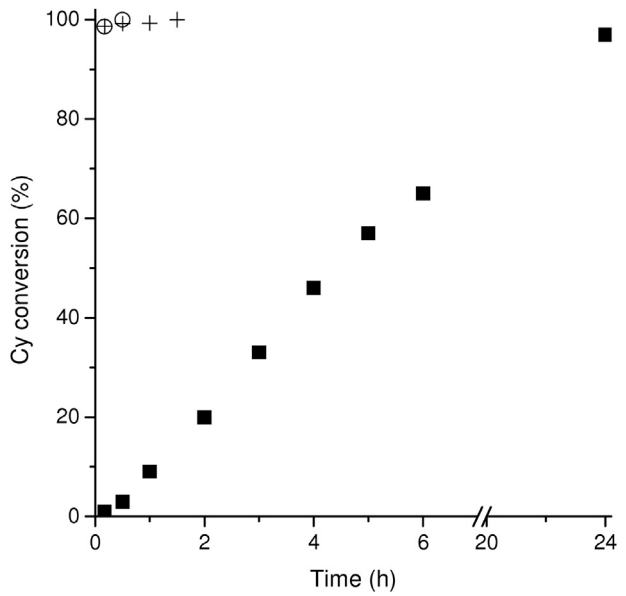

Fig. 7. Kinetic profiles of the catalytic epoxidation of *cis*-cyclooctene (Cy) with TBHP at 55 °C in the presence of **1** (○), **1**/IL (+) and Zn,Al-CpMo (■).

hydroxide, as described above. Under similar reaction conditions to those used for **1** (no cosolvent, 55 °C), CyO was again the only product formed, but the reaction was slower than that observed for the homogeneous catalyst (Fig. 7, Table 1). The initial turnover frequency (determined at 10 min reaction) was 592 and 5 mol mol_{Mo}^{-1} h^{-1} for **1** and Zn,Al-CpMo, respectively, and the latter led to 65%/97% conversion at 6 h/24 h. The different catalytic results for **1** and Zn,Al-CpMo may be partly due to differences in the chemical nature of the metal species and/or diffusion limitations in the case of the intercalated complex (which is a solid–liquid

Table 1
Catalytic epoxidation of *cis*-cyclooctene with TBHP at 55 °C.[a]

Precatalyst	Cosolvent[b]	Catalytic run	Reaction time (h)	Conversion (%)	Epoxide selectivity (%)
1	ns	1	0.5	100	100
	$[bmim]NTf_2$	1	0.17	99	100
	$[bmim]NTf_2$	2	6/24	65/85	100/100
	$[bmim]NTf_2$	3	6/24	26/56	100/100
Zn,Al-CpMo	ns	1	6/24	65/97	100/100
	ns	2	6/24	10/34	100/100
	ns	3	6/24	7/25	100/100

[a] Reaction conditions: Mo:Cy:TBHP molar ratio = 1:100:150, without additional cosolvent, 55 °C.
[b] ns = no cosolvent was added.

biphasic reaction system). After a 24 h batch run, the solid was separated from the reaction mixture by centrifugation, washed with *n*-hexane, dried at room temperature overnight, and characterized by FT-IR spectroscopy (Fig. 1). The bands associated with the carbonyl ligands are reduced to very weak intensity, indicating that extensive decarbonylation of the intercalated complex had taken place. Additionally, one new band at 895 cm^{-1} and a shoulder at ca. 930 cm^{-1} are present, which are assigned to Mo=O stretching vibrations, probably consistent with the formation of a dioxomolybdenum(VI) species. However, despite the formation of oxidized metal species, the reaction rate decreased in consecutive batch runs (Table 1). These results may be partly due to metal leaching, which was checked by carrying out the leaching test (as described in detail in the Experimental section). An increment in conversion between 2 h (instant of the separation of the solid by filtration) and 24 h reaction of 79% was observed for the leaching test, which is similar to the 77% increment observed for the typical catalytic run (without filtration) in the same time interval. Hence, active species were leached from the solid into solution during the catalytic reaction.

4. Concluding remarks

Monomeric cyclopentadienyl molybdenum carbonyl complexes of general formula $(\eta^5\text{-}C_5R_5)Mo(CO)_3X$ are known to be pre-catalysts for olefin epoxidation. In this work, we have found that the complex $CpMo(CO)_3CH_2COOH$ (**1**) is one of the most active compounds in this class, using cyclooctene as a benchmark substrate. Interesting catalytic results were also obtained with α-pinene as substrate, giving the added-value products α-pinene oxide and campholenic aldehyde. To date, various approaches have been reported to facilitate catalyst recycling and reuse using these complexes, such as immobilization in ionic liquids [15,29,40], cyclodextrins [23,28,41] and porous inorganic supports [9,10]. In this work we describe a completely new approach based on the intercalation of the anionic complex in a layered double hydroxide. The resultant inorganic–organometallic hybrid material is of significant interest from a structural point of view due to the high loading of complexes achieved in a bilayer-type arrangement with some evidence for periodic ordering of the guests within the interlayer region. Catalytic results for the epoxidation of cyclooctene were disappointing, despite the fact that the *in situ* oxidative decarbonylation of intercalated complexes (by reaction with TBHP) proceeded almost to completion during the first batch run, resulting in the formation of oxidized metal species. Partial leaching of these species is mainly responsible for the observed catalytic activity, and we may assume that the performance of the material as a heterogeneous catalyst is conditioned by limited access of the substrate to the active sites. Better results in terms of catalytic activity were obtained using the ionic liquid $[bmim]NTf_2$ as solvent. However, the reaction rate decreased in consecutive batch runs, most likely due to the gradual removal of active species during the solvent extraction process. In future work a wider range of ILs will be studied with the aim of achieving better catalytic results with the title compound $CpMo(CO)_3CH_2COOH$.

Acknowledgments

We are grateful to the Fundação para a Ciência e a Tecnologia (FCT), QREN, Fundo Europeu de Desenvolvimento Regional (FEDER), COMPETE, the European Union, the Associate Laboratory CICECO (PEst-C/CTM/LA0011/2013) and CQE (PEst-OE/QUI/UI0100/2013) for continued support and funding, including the R&D Project PTDC/QEQ-SUP/1906/2012 and the research grant BPD/UI89/4864/2013 (A.C.G.) provided within this project. The NMR spectrometers are part of The National NMR Network (REDE/1517/RMN/2005), supported by POCI 2010 and the FCT. The authors also thank the Portuguese NMR Network (IST-UTL Center) (RECI/QEQ-QIN/0189/2012) for providing access to the NMR facilities. The FCT and the European Union are acknowledged for a post-doctoral grant to S.M.B (SFRH/BPD/46473/2008) cofunded by MEC and the European Social Fund through the program POPH of QREN.

References

[1] S.A. Hauser, M. Cokoja, F.E. Kühn, Catal. Sci. Technol. 3 (2013) 552.
[2] S. Huber, M. Cokoja, F.E. Kühn, J. Organomet. Chem. (2013) in press.
[3] H. Srour, P.L. Maux, S. Chevance, G. Simonneaux, Coord. Chem. Rev. 257 (2013) 3030.
[4] J.-M. Brégeault, J. Chem. Soc. Dalton Trans. (2003) 3289.
[5] M.N. Sheng, J.G. Zajacek, ARCO, GB Patent 1,136,923, 1968.
[6] J. Kollar, Halcon, US Patent 3,351,635, 1967.
[7] N. Grover, F.E. Kühn, Curr. Org. Chem. 16 (2012) 16.
[8] T. Szymańska-Buzar, Curr. Org. Chem. 16 (2012) 3.
[9] K.R. Jain, F.E. Kühn, Dalton Trans. (2008) 2221.
[10] P.D. Vaz, C.D. Nunes, Curr. Org. Chem. 16 (2012) 89.
[11] M. Abrantes, A. Sakthivel, C.C. Romão, F.E. Kühn, J. Organomet. Chem. 691 (2006) 3137.
[12] M. Abrantes, F.A.A. Paz, A.A. Valente, C.C.L. Pereira, S. Gago, A.E. Rodrigues, J. Klinowski, M. Pillinger, I.S. Gonçalves, J. Organomet. Chem. 694 (2009) 1826.
[13] M. Abrantes, A.M. Santos, J. Mink, F.E. Kühn, C.C. Romão, Organometallics 22 (2003) 2112.
[14] D. Betz, A. Raith, M. Cokoja, F.E. Kühn, ChemSusChem 3 (2010) 559.
[15] S.A. Hauser, M. Cokoja, M. Drees, F.E. Kühn, J. Mol. Catal. A Chem. 363–364 (2012) 237.
[16] A.M. Martins, C.C. Romão, M. Abrantes, M.C. Azevedo, J. Cui, A.R. Dias, M.T. Duarte, M.A. Lemos, T. Lourenço, R. Poli, Organometallics 24 (2005) 2582.
[17] P.J. Costa, M.J. Calhorda, F.E. Kühn, Organometallics 29 (2010) 303.
[18] M.J. Calhorda, P.J. Costa, Curr. Org. Chem. 16 (2012) 65.
[19] A.C. Gomes, S.M. Bruno, C.A. Gamelas, A.A. Valente, M. Abrantes, I.S. Gonçalves, C.C. Romão, M. Pillinger, Dalton Trans. 42 (2013) 8231.
[20] J.K.P. Ariyaratne, A.M. Bierrum, M.L.H. Green, M. Ishaq, C.K. Prout, M.G. Swanwick, J. Chem. Soc. A (1969) 1309.
[21] A.C. Gomes, S.M. Bruno, A.A. Valente, I.S. Gonçalves, M. Pillinger, J. Organomet. Chem. 744 (2013) 53.
[22] M. Abrantes, S. Gago, A.A. Valente, M. Pillinger, I.S. Gonçalves, T.M. Santos, J. Rocha, C.C. Romão, Eur. J. Inorg. Chem. (2004) 4914.
[23] S.S. Braga, S. Gago, J.D. Seixas, A.A. Valente, M. Pillinger, T.M. Santos, I.S. Gonçalves, C.C. Romão, Inorg. Chim. Acta 359 (2006) 4757.
[24] J.T. Kloprogge, L. Hickey, R.L. Frost, J. Solid State Chem. 177 (2004) 4047.
[25] S. Gago, M. Pillinger, T.M. Santos, J. Rocha, I.S. Gonçalves, Eur. J. Inorg. Chem. (2004) 1389.
[26] M. Bellotto, B. Rebours, O. Clause, J. Lynch, D. Bazin, E. Elkaïm, J. Phys. Chem. 100 (1996) 8527.
[27] F. Thevenot, R. Szymanski, P. Chaumette, Clays Clay Miner. 37 (1989) 396.
[28] A.C. Gomes, S.M. Bruno, C. Tomé, A.A. Valente, M. Pillinger, M. Abrantes, I.S. Gonçalves, J. Organomet. Chem. 730 (2013) 116.
[29] M. Abrantes, P. Neves, M.M. Antunes, S. Gago, F.A.A. Paz, A.E. Rodrigues, M. Pillinger, I.S. Gonçalves, C.M. Silva, A.A. Valente, J. Mol. Catal. A Chem. 320 (2010) 19.
[30] A.A. Valente, J.D. Seixas, I.S. Gonçalves, M. Abrantes, M. Pillinger, C.C. Romão, Catal. Lett. 101 (2005) 127.
[31] J. Zhao, A.M. Santos, E. Herdtweck, F.E. Kühn, J. Mol. Catal. A Chem. 222 (2004) 265.
[32] J. Zhao, E. Herdtweck, F.E. Kühn, J. Organomet. Chem. 691 (2006) 2199.
[33] J. Zhao, K.R. Jain, E. Herdtweck, F.E. Kühn, Dalton Trans. (2007) 5567.
[34] A. Capapé, A. Raith, F.E. Kühn, Adv. Synth. Catal. 351 (2009) 66.
[35] A. Capapé, A. Raith, E. Herdtweck, M. Cokoja, F.E. Kühn, Adv. Synth. Catal. 352 (2010) 547.
[36] I.O. Jawonisi, G.I. Adoga, Br. J. Pharmacol. Toxicol. 4 (2013) 155.
[37] V.V. Costa, K.A. da Silva Rocha, L.F. de Sousa, P.A. Robles-Dutenhefner, E.V. Gusevskay, J. Mol. Catal. A Chem. 345 (2011) 69.
[38] I.V. Il'ina, K.P. Volcho, N.F. Salakhutdinov, Russ. J. Org. Chem. 44 (2008) 1.
[39] W.F. Holderich, J. Roseler, G. Heitmann, A.T. Liebens, Catal. Today 37 (1997) 353.
[40] F.E. Kühn, J. Zhao, M. Abrantes, W. Sun, C.A.M. Afonso, L.C. Branco, I.S. Gonçalves, M. Pillinger, C.C. Romão, Tetrahedron Lett. 46 (2005) 47.
[41] S.S. Balula, A.C. Coelho, S.S. Braga, A. Hazell, A.A. Valente, M. Pillinger, J.D. Seixas, C.C. Romão, I.S. Gonçalves, Organometallics 26 (2007) 6857.